Figure 1

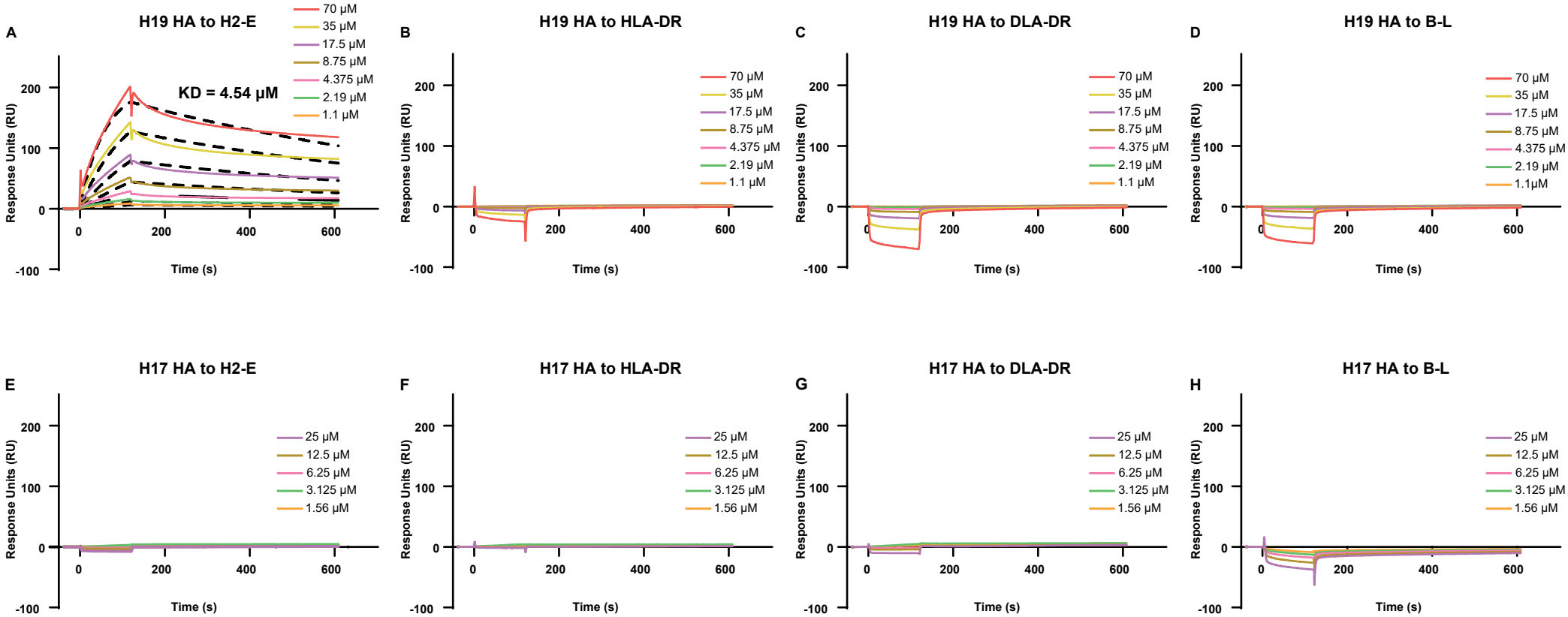
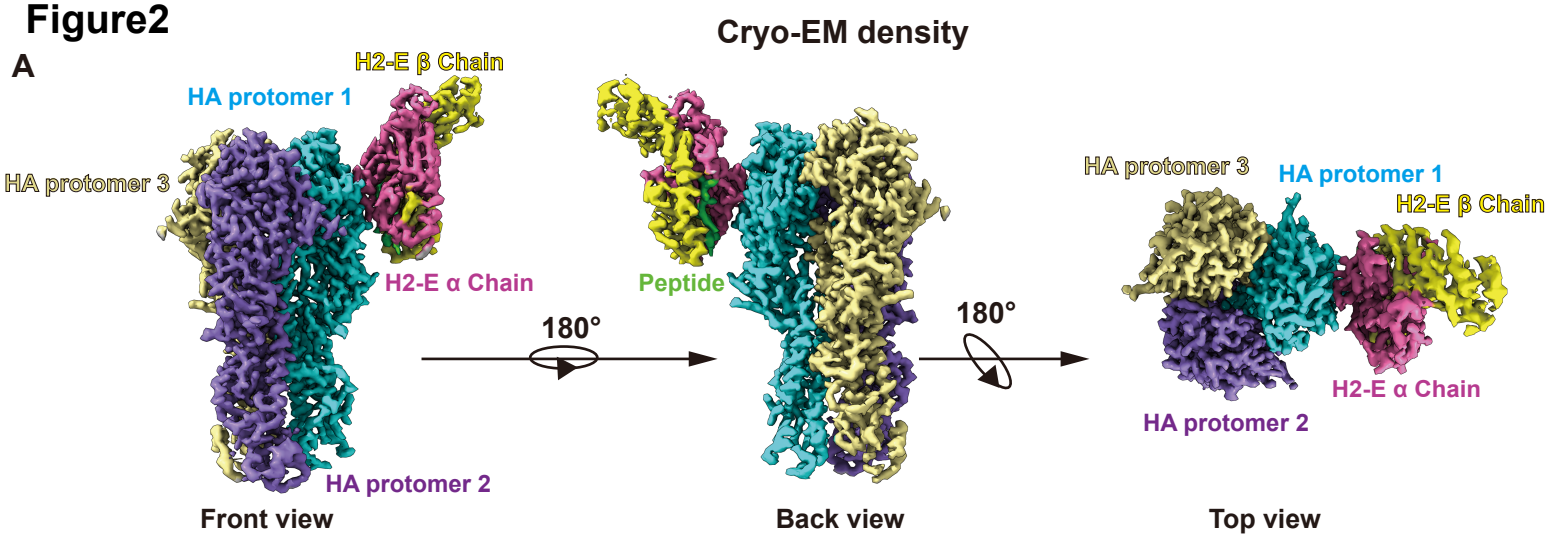
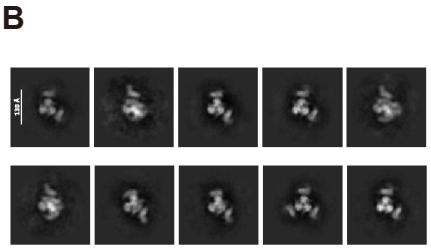
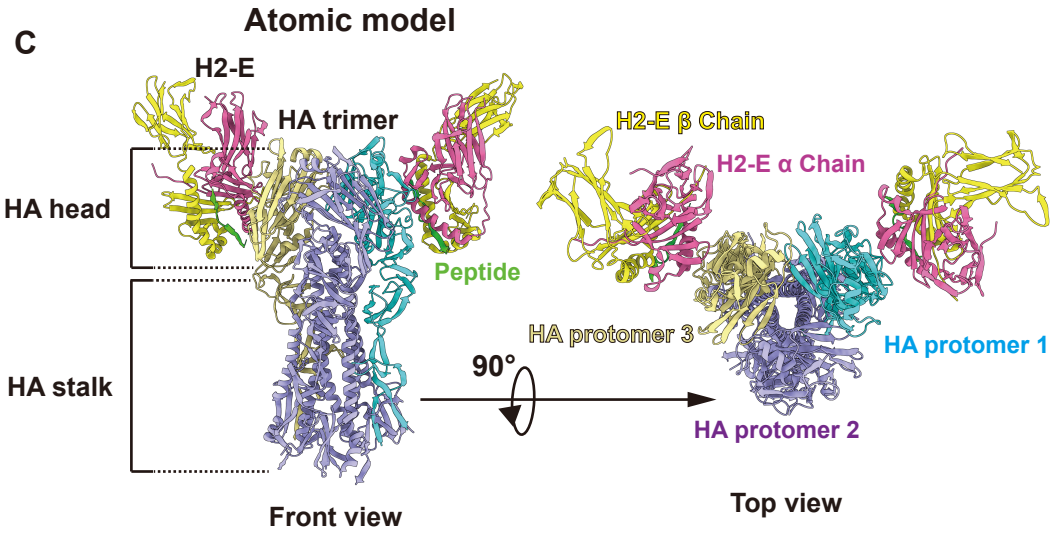

A
H19 HA to H2-E
KD = 4.54 μM
70 μM
35 μM
17.5 μM
8.75 μM
4.375 μM
2.19 μM
1.1 μM
Response Units (RU)
Time (s)
B
H19 HA to HLA-DR
C
H19 HA to DLA-DR
D
H19 HA to B-L
1.1μM
E
H17 HA to H2-E
25 μM
12.5 μM
6.25 μM
3.125 μM
1.56 μM
F
H17 HA to HLA-DR
G
H17 HA to DLA-DR
H
H17 HA to B-L

Figure2


A
Cryo-EM density
H2-E β Chain
HA protomer 1
HA protomer 3
H2-E α Chain
HA protomer 2
Front view
180°
Peptide
Back view
180°
HA protomer 3
HA protomer 1
H2-E β Chain
H2-E α Chain
HA protomer 2
Top view


B


C
Atomic model
H2-E
HA trimer
HA head
HA stalk
Peptide
Front view
H2-E β Chain
H2-E α Chain
HA protomer 3
HA protomer 1
90°
HA protomer 2
Top view

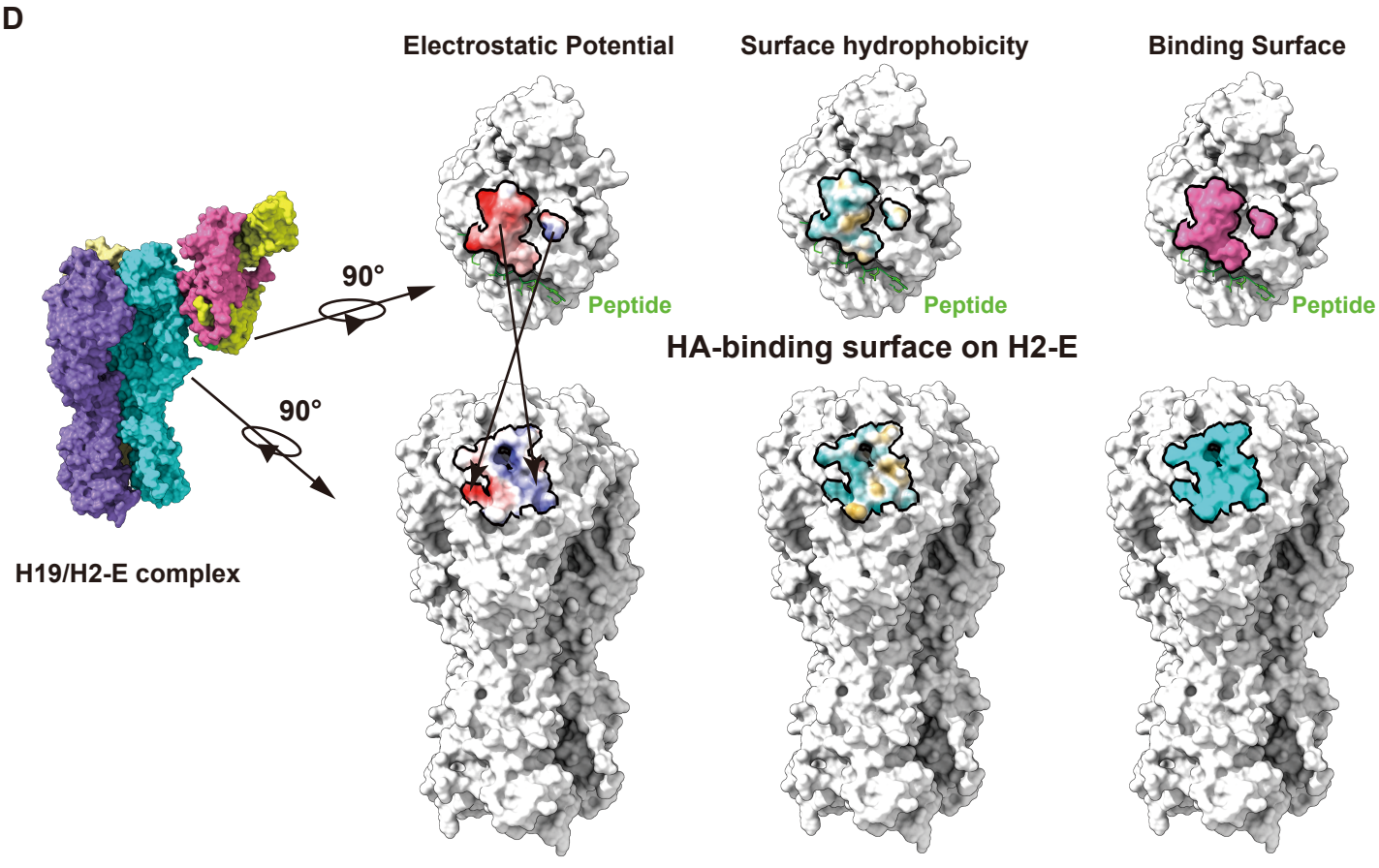

D
Electrostatic Potential
Surface hydrophobicity
Binding Surface
90°
90°
Peptide
Peptide
Peptide
HA-binding surface on H2-E
H19/H2-E complex
H2-E-binding surface on HA

Figure 3

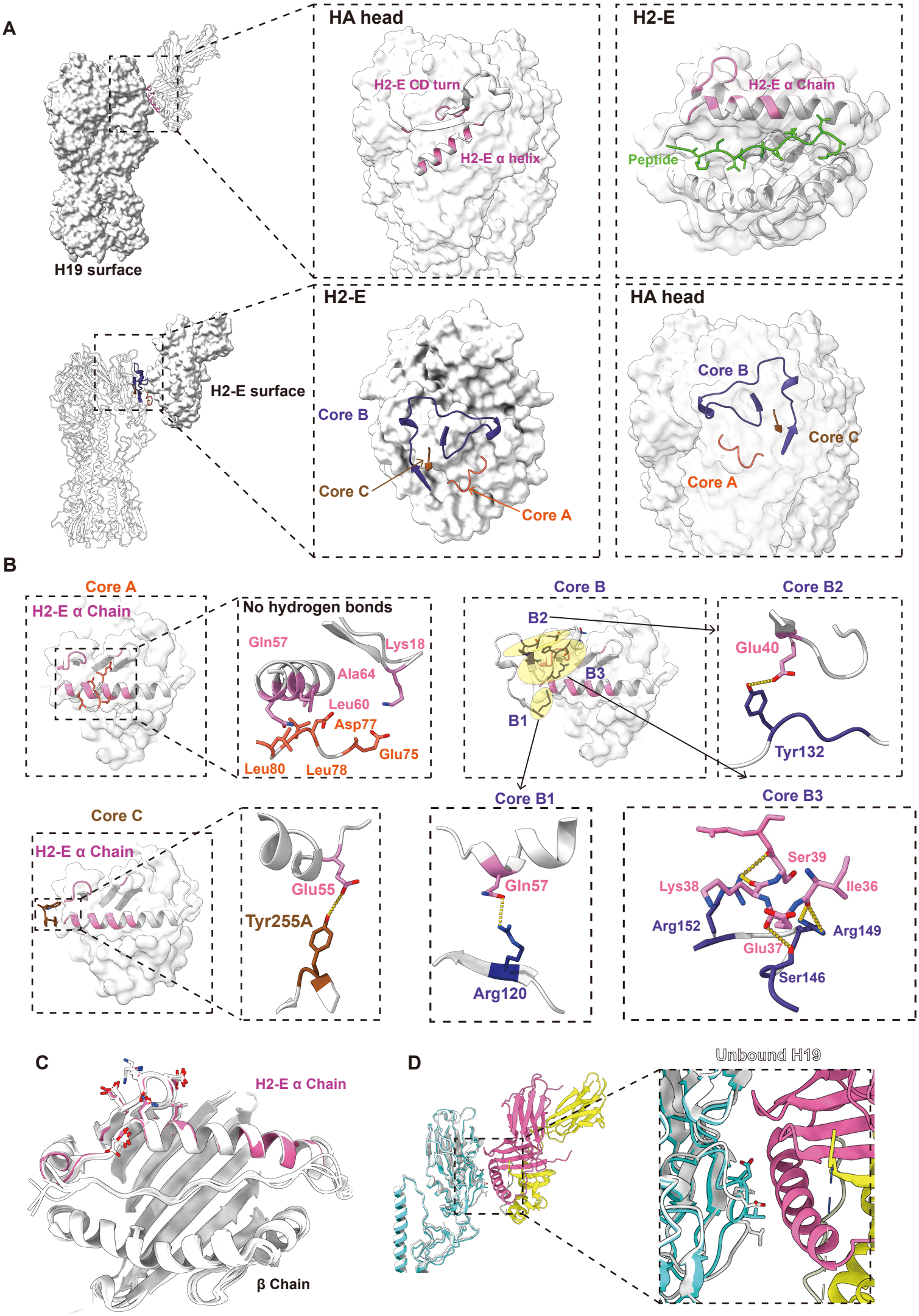
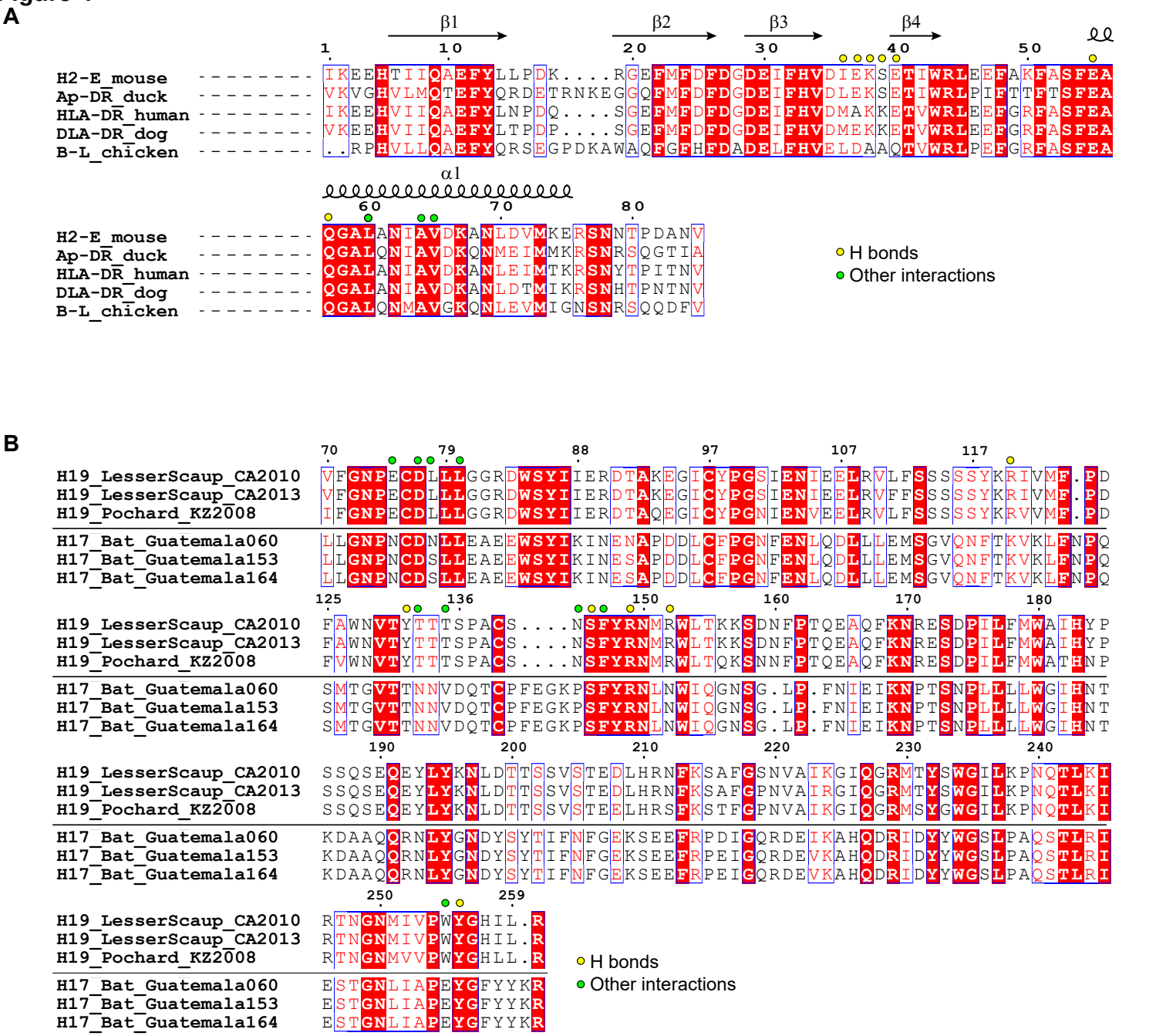

A
H19 surface
HA head
H2-E CD turn
H2-E α helix
H2-E
H2-E α Chain
Peptide
H2-E surface
H2-E
Core B
Core C
Core A
HA head
Core B
Core C
Core A
B
Core A
H2-E α Chain
No hydrogen bonds
Gln57
Lys18
Ala64
Leu60
Asp77
Glu75
Leu80
Leu78
Core B
B2
B3
B1
Core B2
Glu40
Tyr132
Core C
H2-E α Chain
Glu55
Tyr255A
Core B1
Gln57
Arg120
Core B3
Ser39
Lys38
Ile36
Arg152
Arg149
Glu37
Ser146
C
H2-E α Chain
β Chain
D
Unbound H19

Figure 4



C

MHC II α chain variation at the H19 interface

	57	40	37	36	38	39	55
H2-E (mouse)	Q	E	E	I	K	S	E
HLA-DR (human)	Q	E	A	M	K	K	E
DLA-DR (dog)	Q	E	E	M	K	K	E
B-L (chicken)	Q	Q	D	L	A	A	E
H19	R 120	Y 132	S 146	R 149	R 152	R 152	Y 255A

D

HA variation at the H2-E interface

	120	132	146	149	152	152	255A
H19	R	Y	S	R	R	R	Y
H18	K	T	S	R	N	N	Y
H17	K	T	S	R	N	N	Y
H2-E	Q 57	E 40	E 37	I 36	K 38	S 39	E 55

Figure 5

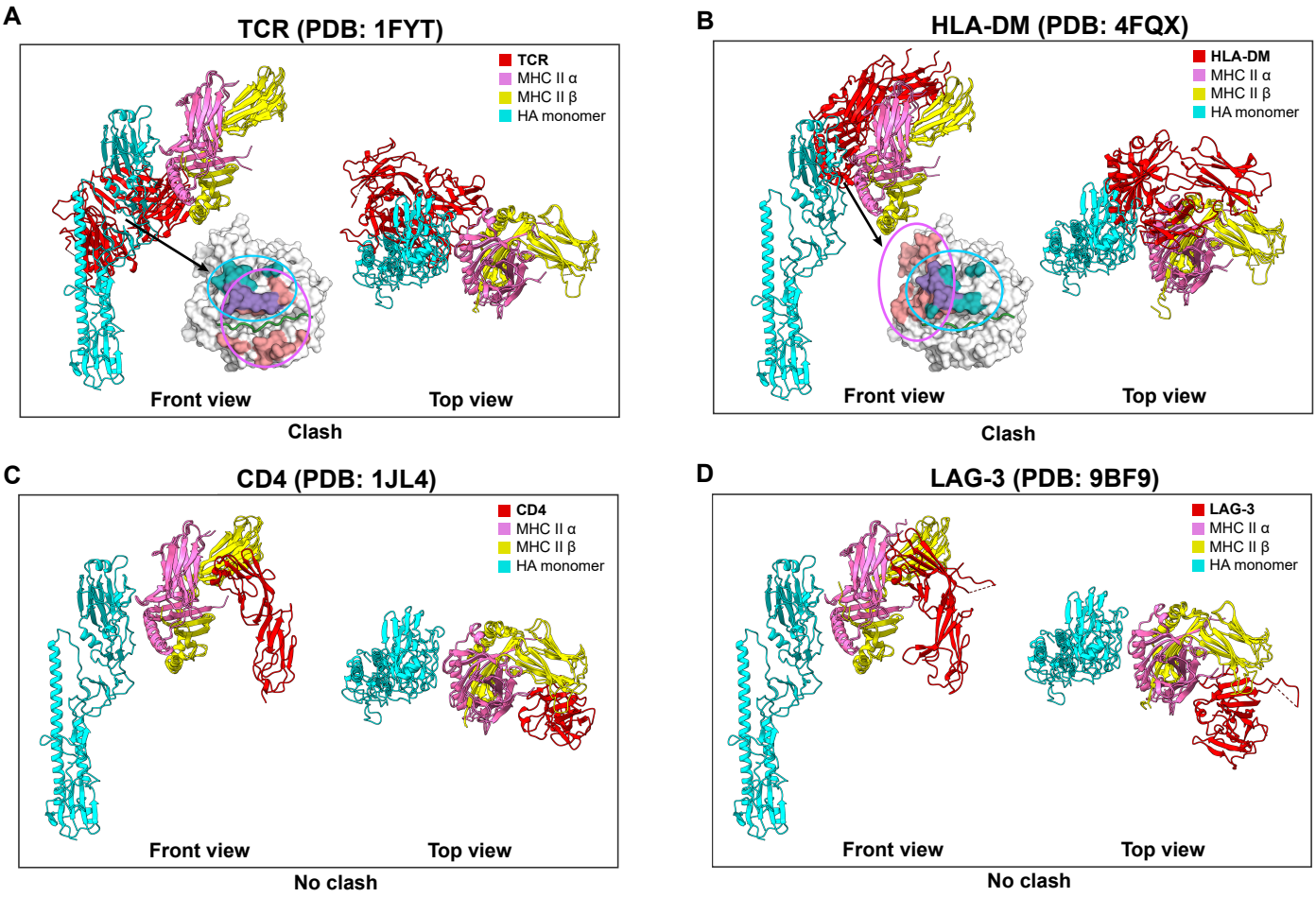

A
TCR (PDB: 1FYT)
TCR
MHC II α
MHC II β
HA monomer
Front view
Top view
Clash
B
HLA-DM (PDB: 4FQX)
HLA-DM
MHC II α
MHC II β
HA monomer
Front view
Top view
Clash
C
CD4 (PDB: 1JL4)
CD4
MHC II α
MHC II β
HA monomer
Front view
Top view
No clash
D
LAG-3 (PDB: 9BF9)
LAG-3
MHC II α
MHC II β
HA monomer
Front view
Top view
No clash

Figure S1

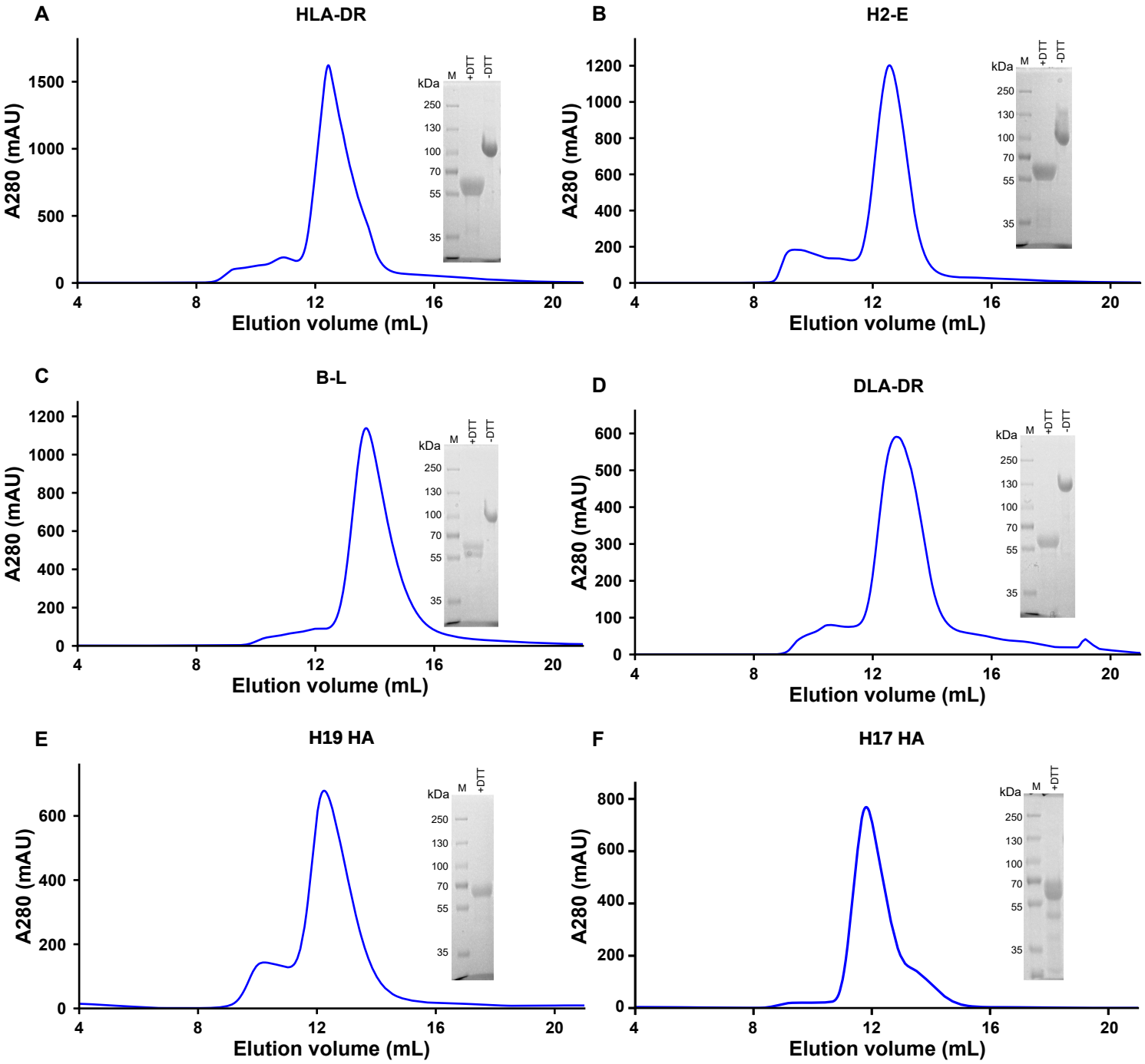
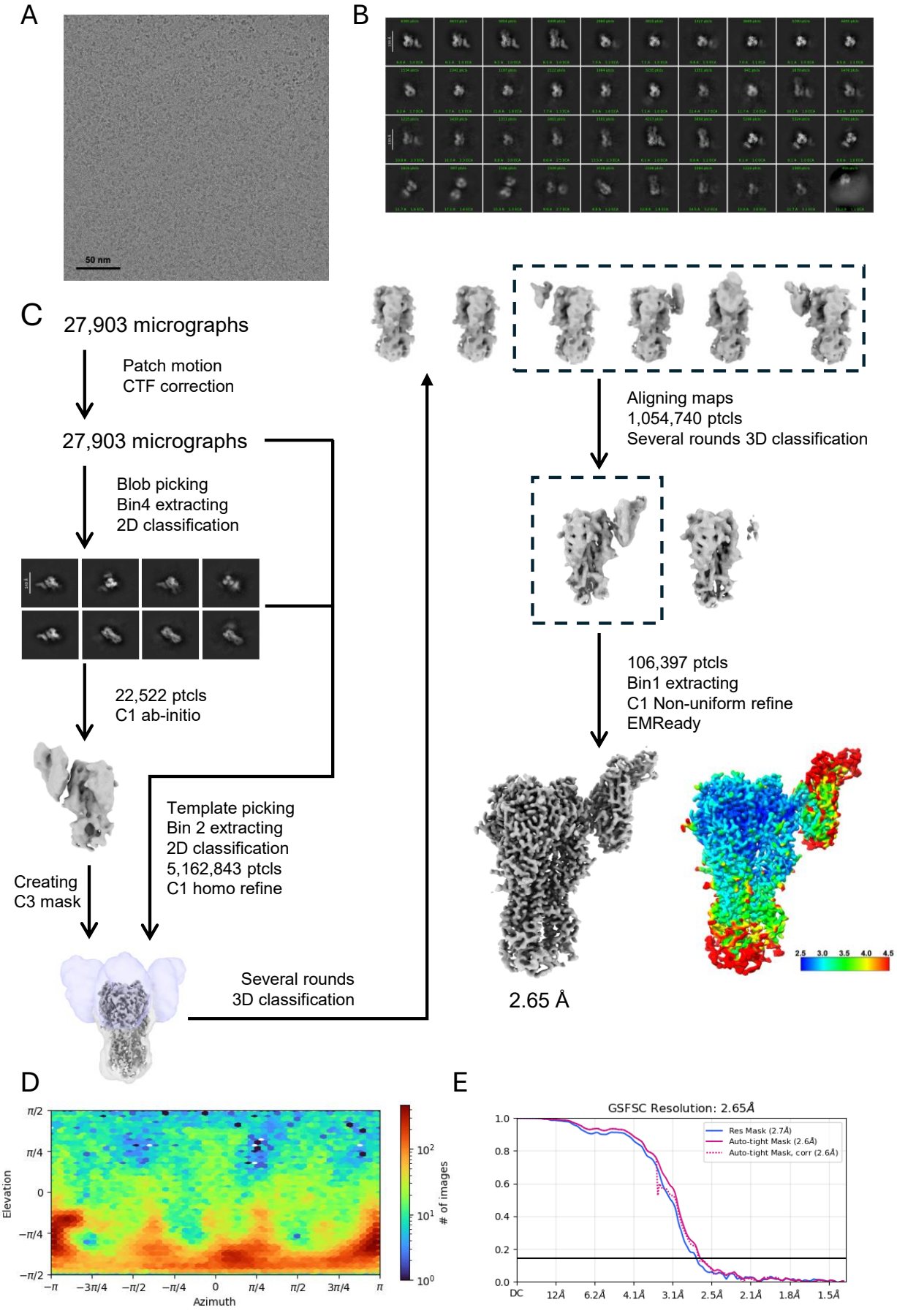
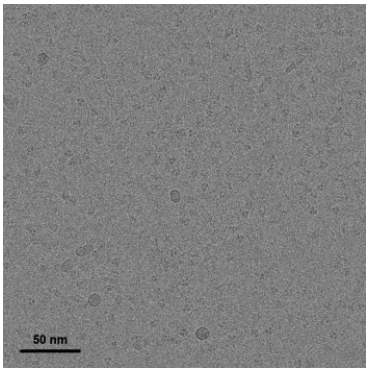

A
HLA-DR
A280 (mAU)
Elution volume (mL)
kDa
M
+DTT
-DTT
250
130
100
70
55
35
B
H2-E
C
B-L
D
DLA-DR
E
H19 HA
F
H17 HA

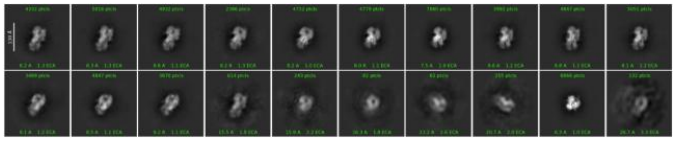
Figure S2

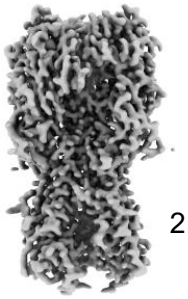

A
50 nm
B
C
27,903 micrographs
Patch motion
CTF correction
27,903 micrographs
Blob picking
Bin4 extracting
2D classification
22,522 ptcls
C1 ab-initio
Creating
C3 mask
Template picking
Bin 2 extracting
2D classification
5,162,843 ptcls
C1 homo refine
Several rounds
3D classification
Aligning maps
1,054,740 ptcls
Several rounds 3D classification
106,397 ptcls
Bin1 extracting
C1 Non-uniform refine
EMReady
2.5 3.0 3.5 4.0 4.5
2.65 Å
D
Elevation
Azimuth
# of images
E
GSFSC Resolution: 2.65Å
Res Mask (2.7Å)
Auto-tight Mask (2.6Å)
Auto-tight Mask, corr (2.6Å)
DC
12Å
6.2Å
4.1Å
3.1Å
2.5Å
2.1Å
1.8Å
1.5Å

F

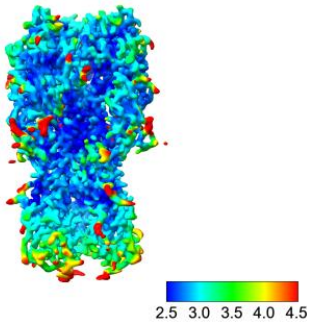


G





2.69 Å



H

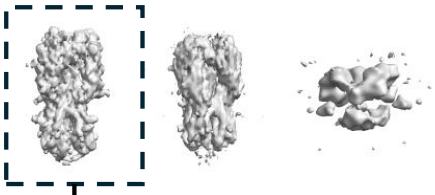
14,346 micrographs

Patch motion
CTF correction

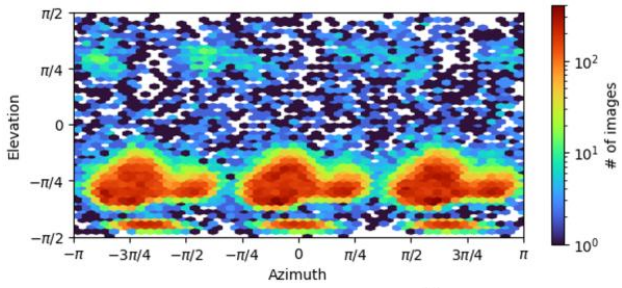
14,346 micrographs

Blob picking
3*2D classification
Template picking
3*2D classification
201,912 ptcls
C3 ab-initio
C3 Heter refine

C3 Non-uniform refine
C3 Homo refine
68,265 ptcls
Rebalance orientation
C3 Homo refine
146,108 ptcls



I



J

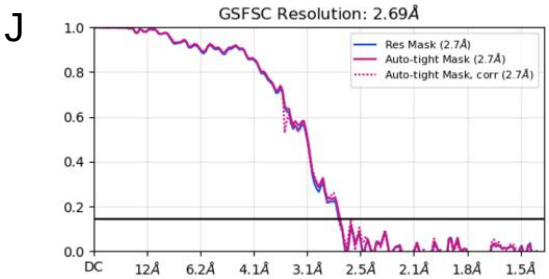
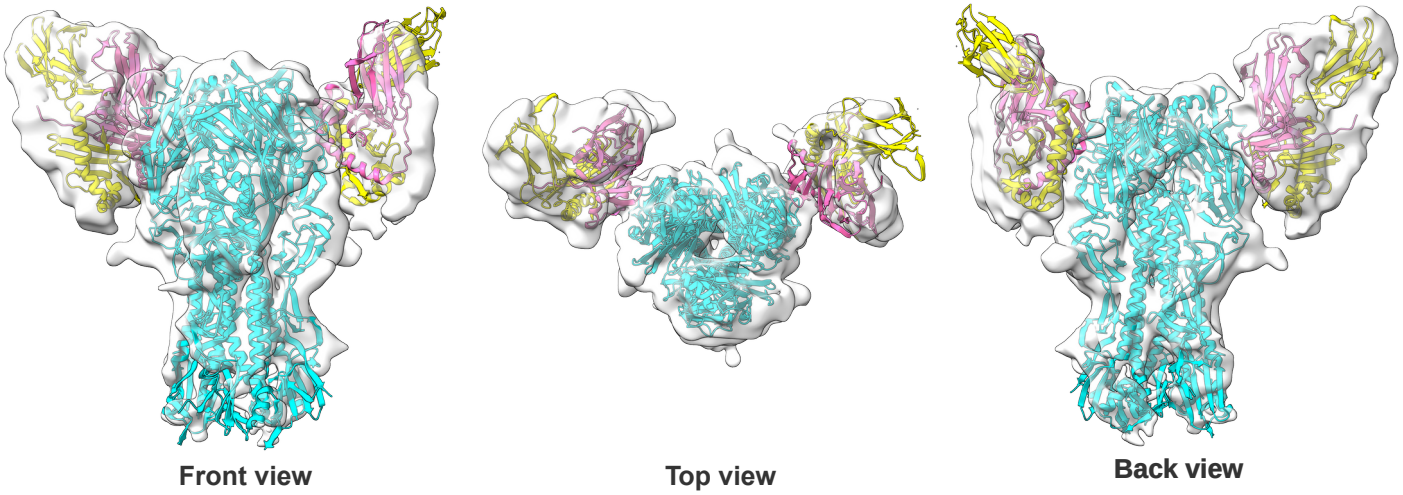


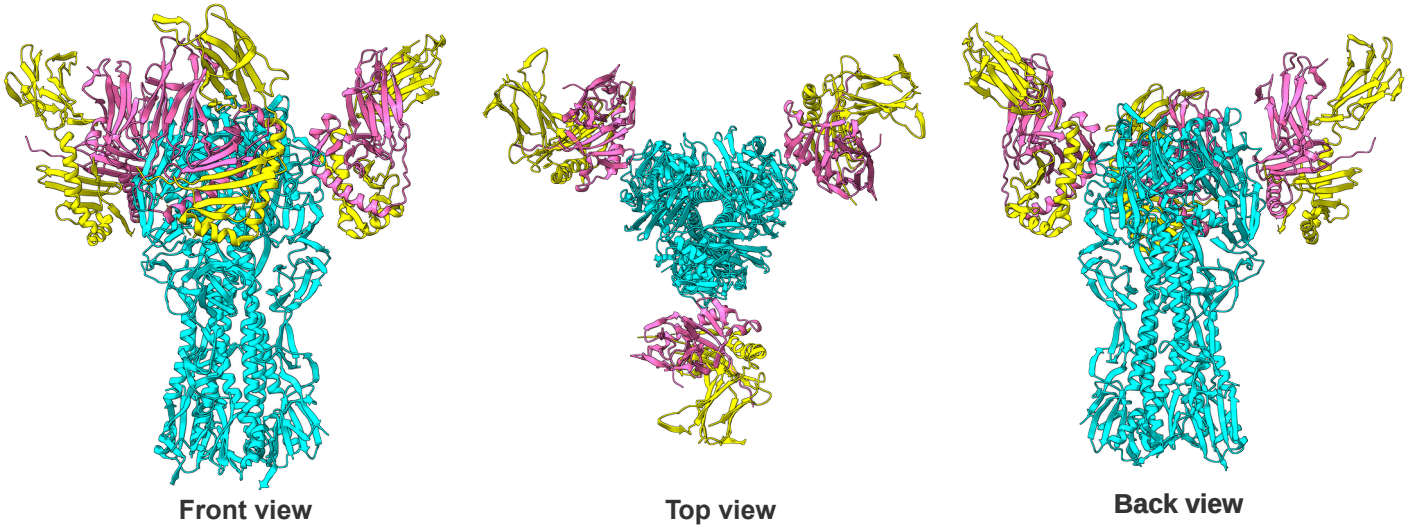
Figure S3

A



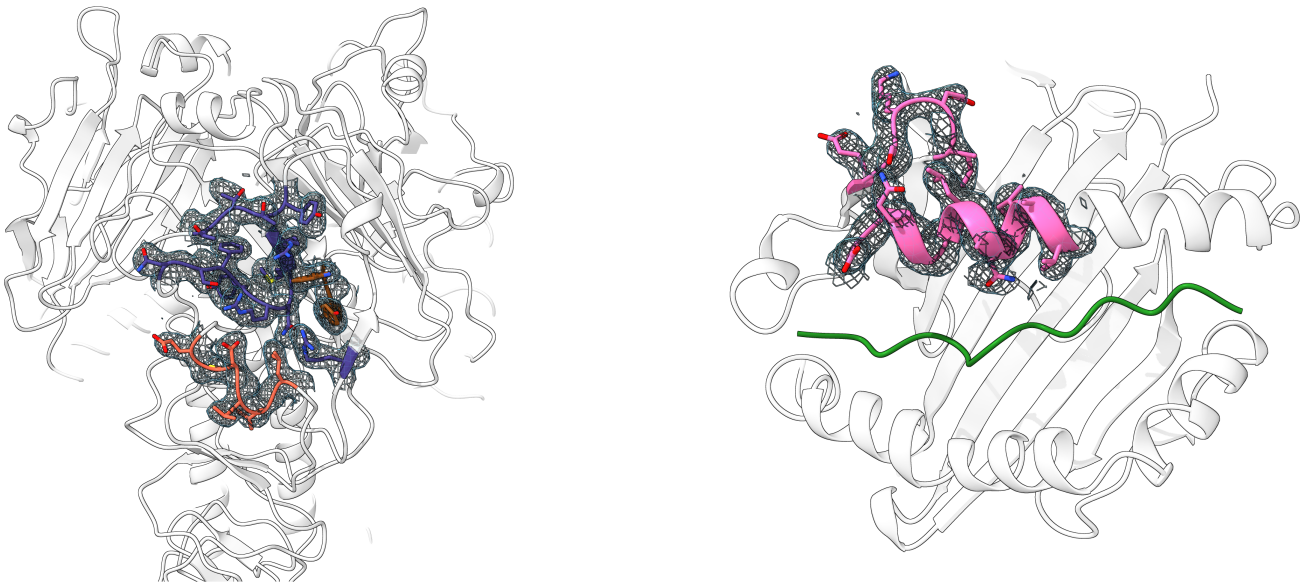
Cryo-EM density of the 2 H2-E bound complex at 6.06 Å

B



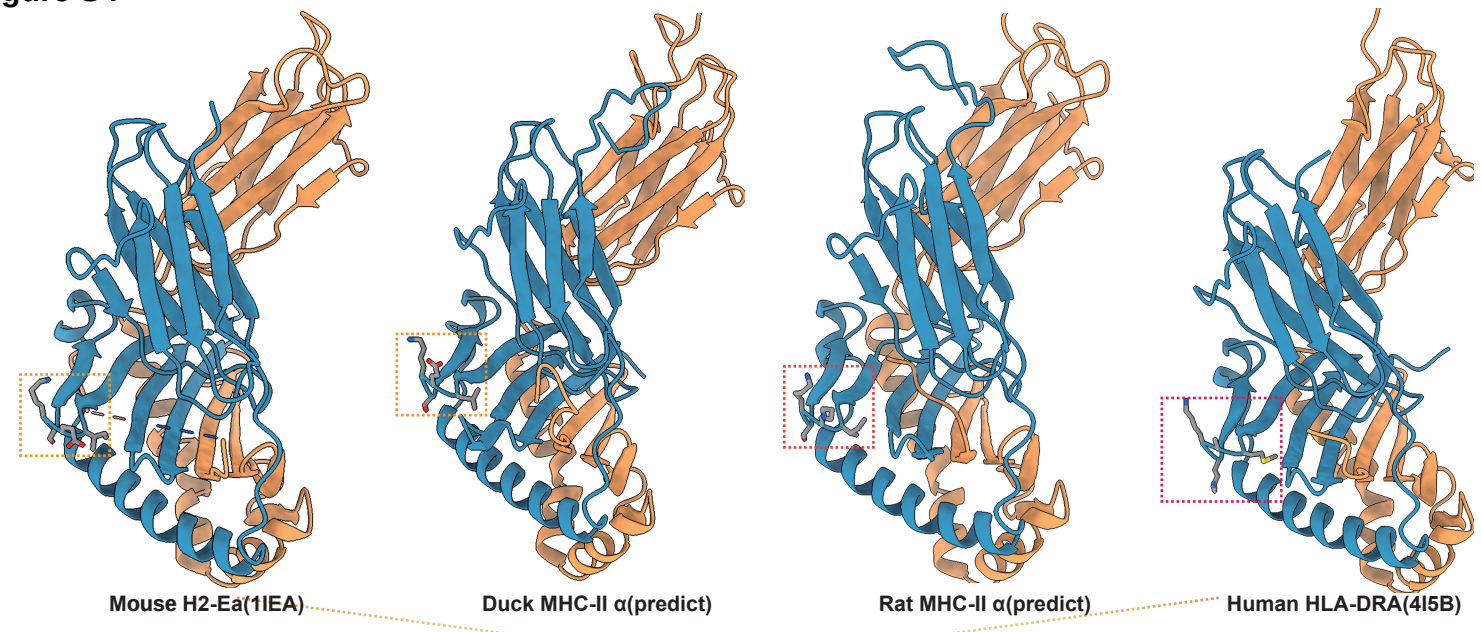
Single H2-E bound complex-based modeling

C



The cryo-EM density at the H19/H2-E interface

Figure S4


Mouse H2-Ea(1IEA)
Duck MHC-II α(predict)
Rat MHC-II α(predict)
Human HLA-DRA(4I5B)

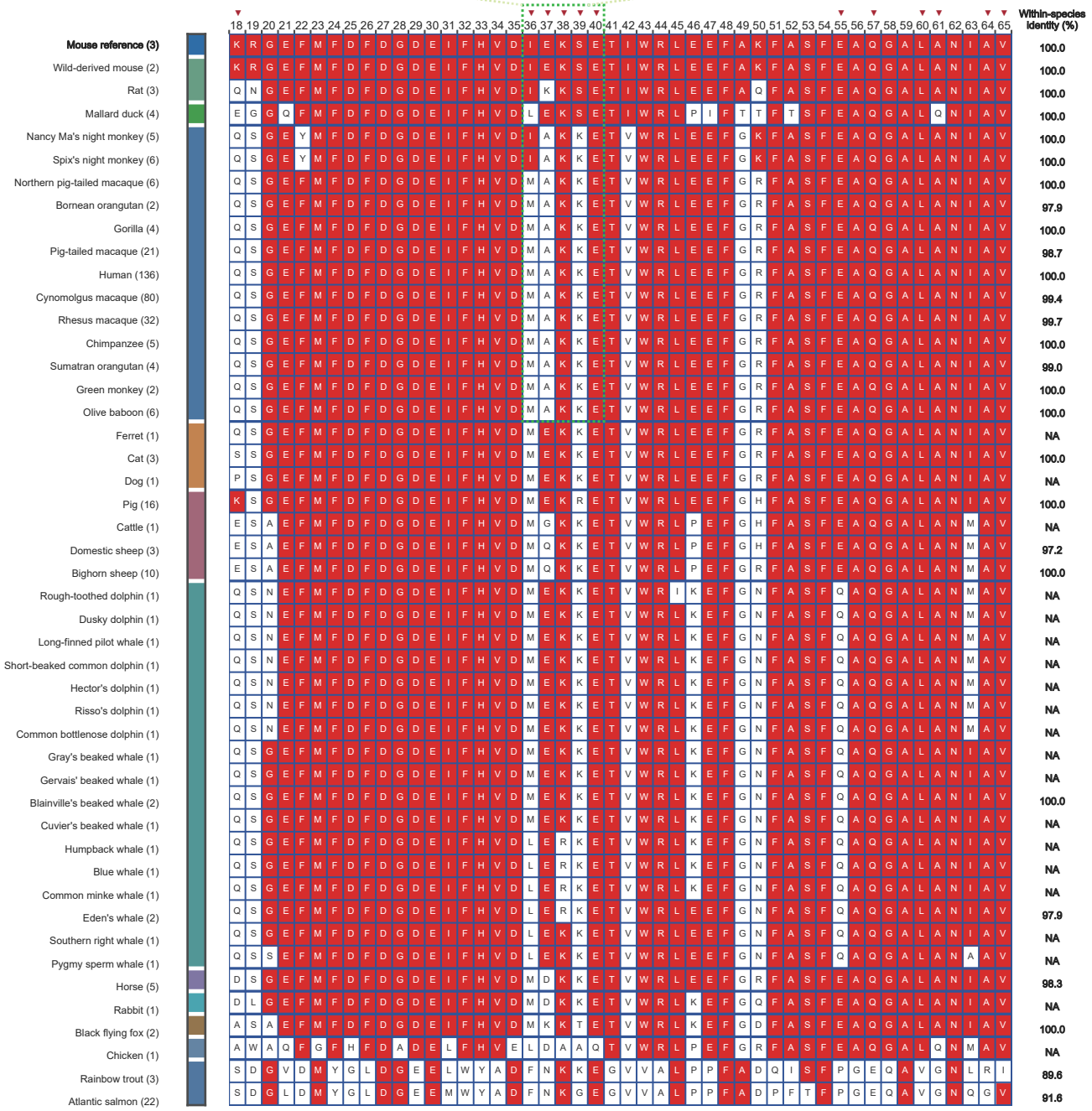
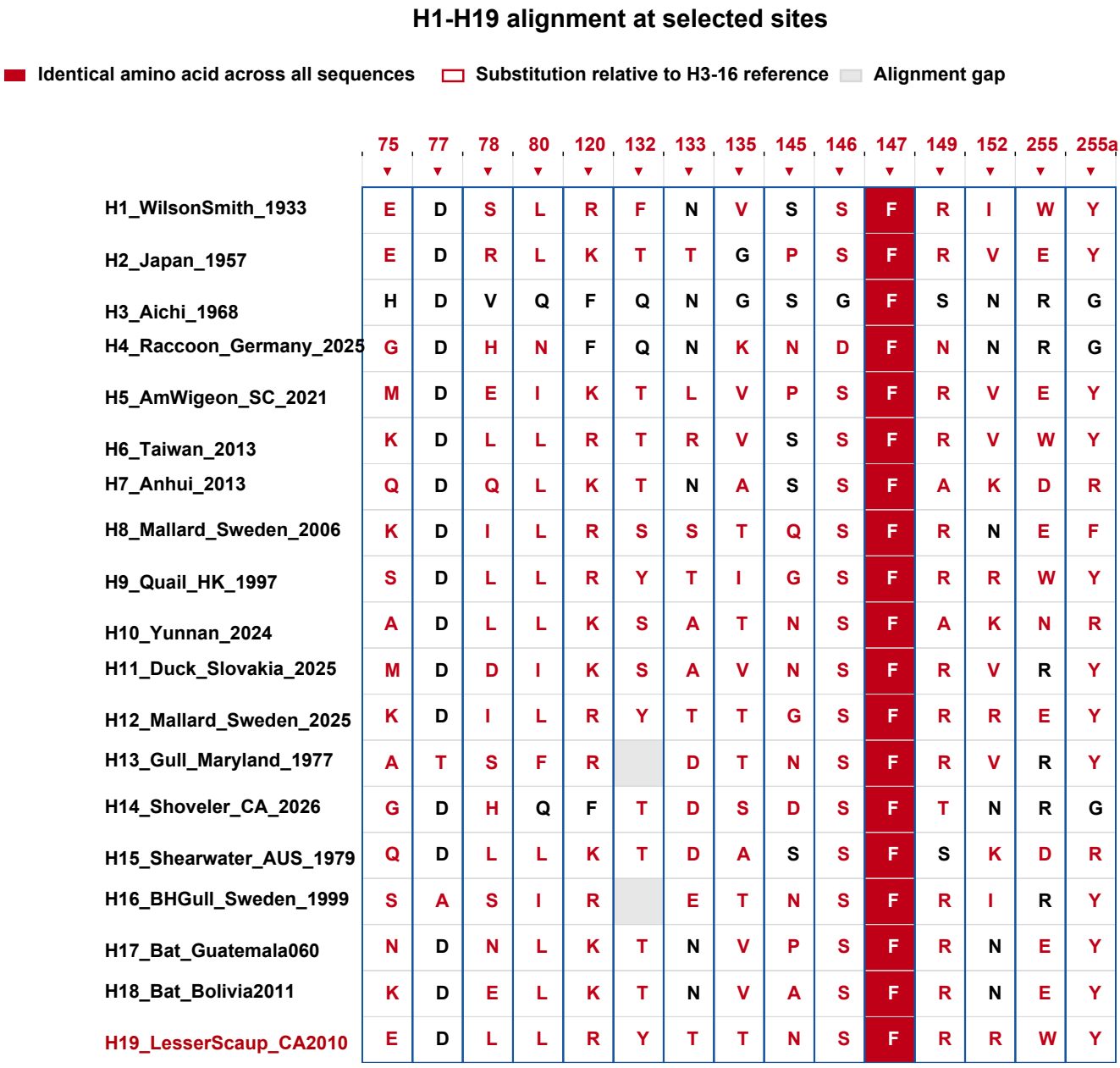

18 19 20 21 22 23 24 25 26 27 28 29 30 31 32 33 34 35 36 37 38 39 40 41 42 43 44 45 46 47 48 49 50 51 52 53 54 55 56 57 58 59 60 61 62 63 64 65
Within-species Identity (%)
Mouse reference (3) 100.0
Wild-derived mouse (2) 100.0
Rat (3) 100.0
Mallard duck (4) 100.0
Nancy Ma's night monkey (5) 100.0
Spix's night monkey (6) 100.0
Northern pig-tailed macaque (6) 100.0
Bornean orangutan (2) 97.9
Gorilla (4) 100.0
Pig-tailed macaque (21) 98.7
Human (136) 100.0
Cynomolgus macaque (80) 99.4
Rhesus macaque (32) 99.7
Chimpanzee (5) 100.0
Sumatran orangutan (4) 99.0
Green monkey (2) 100.0
Olive baboon (6) 100.0
Ferret (1) NA
Cat (3) 100.0
Dog (1) NA
Pig (16) 100.0
Cattle (1) NA
Domestic sheep (3) 97.2
Bighorn sheep (10) 100.0
Rough-toothed dolphin (1) NA
Dusky dolphin (1) NA
Long-finned pilot whale (1) NA
Short-beaked common dolphin (1) NA
Hector's dolphin (1) NA
Risso's dolphin (1) NA
Common bottlenose dolphin (1) NA
Gray's beaked whale (1) NA
Gervais' beaked whale (1) NA
Blainville's beaked whale (2) 100.0
Cuvier's beaked whale (1) NA
Humpback whale (1) NA
Blue whale (1) NA
Common minke whale (1) NA
Eden's whale (2) 97.9
Southern right whale (1) NA
Pygmy sperm whale (1) NA
Horse (5) 98.3
Rabbit (1) NA
Black flying fox (2) 100.0
Chicken (1) NA
Rainbow trout (3) 89.6
Atlantic salmon (22) 91.6

Figure S5



	75	77	78	80	120	132	133	135	145	146	147	149	152	255	255a
H1_WilsonSmith_1933	E	D	S	L	R	F	N	V	S	S	F	R	I	W	Y
H2_Japan_1957	E	D	R	L	K	T	T	G	P	S	F	R	V	E	Y
H3_Aichi_1968	H	D	V	Q	F	Q	N	G	S	G	F	S	N	R	G
H4_Raccoon_Germany_2025	G	D	H	N	F	Q	N	K	N	D	F	N	N	R	G
H5_AmWigeon_SC_2021	M	D	E	I	K	T	L	V	P	S	F	R	V	E	Y
H6_Taiwan_2013	K	D	L	L	R	T	R	V	S	S	F	R	V	W	Y
H7_Anhui_2013	Q	D	Q	L	K	T	N	A	S	S	F	A	K	D	R
H8_Mallard_Sweden_2006	K	D	I	L	R	S	S	T	Q	S	F	R	N	E	F
H9_Quail_HK_1997	S	D	L	L	R	Y	T	I	G	S	F	R	R	W	Y
H10_Yunnan_2024	A	D	L	L	K	S	A	T	N	S	F	A	K	N	R
H11_Duck_Slovakia_2025	M	D	D	I	K	S	A	V	N	S	F	R	V	R	Y
H12_Mallard_Sweden_2025	K	D	I	L	R	Y	T	T	G	S	F	R	R	E	Y
H13_Gull_Maryland_1977	A	T	S	F	R		D	T	N	S	F	R	V	R	Y
H14_Shoveler_CA_2026	G	D	H	Q	F	T	D	S	D	S	F	T	N	R	G
H15_Shearwater_AUS_1979	Q	D	L	L	K	T	D	A	S	S	F	S	K	D	R
H16_BHGull_Sweden_1999	S	A	S	I	R		E	T	N	S	F	R	I	R	Y
H17_Bat_Guatemala060	N	D	N	L	K	T	N	V	P	S	F	R	N	E	Y
H18_Bat_Bolivia2011	K	D	E	L	K	T	N	V	A	S	F	R	N	E	Y
H19_LesserScaup_CA2010	E	D	L	L	R	Y	T	T	N	S	F	R	R	W	Y

Figure S6

H1-H19 hemagglutinin alignment

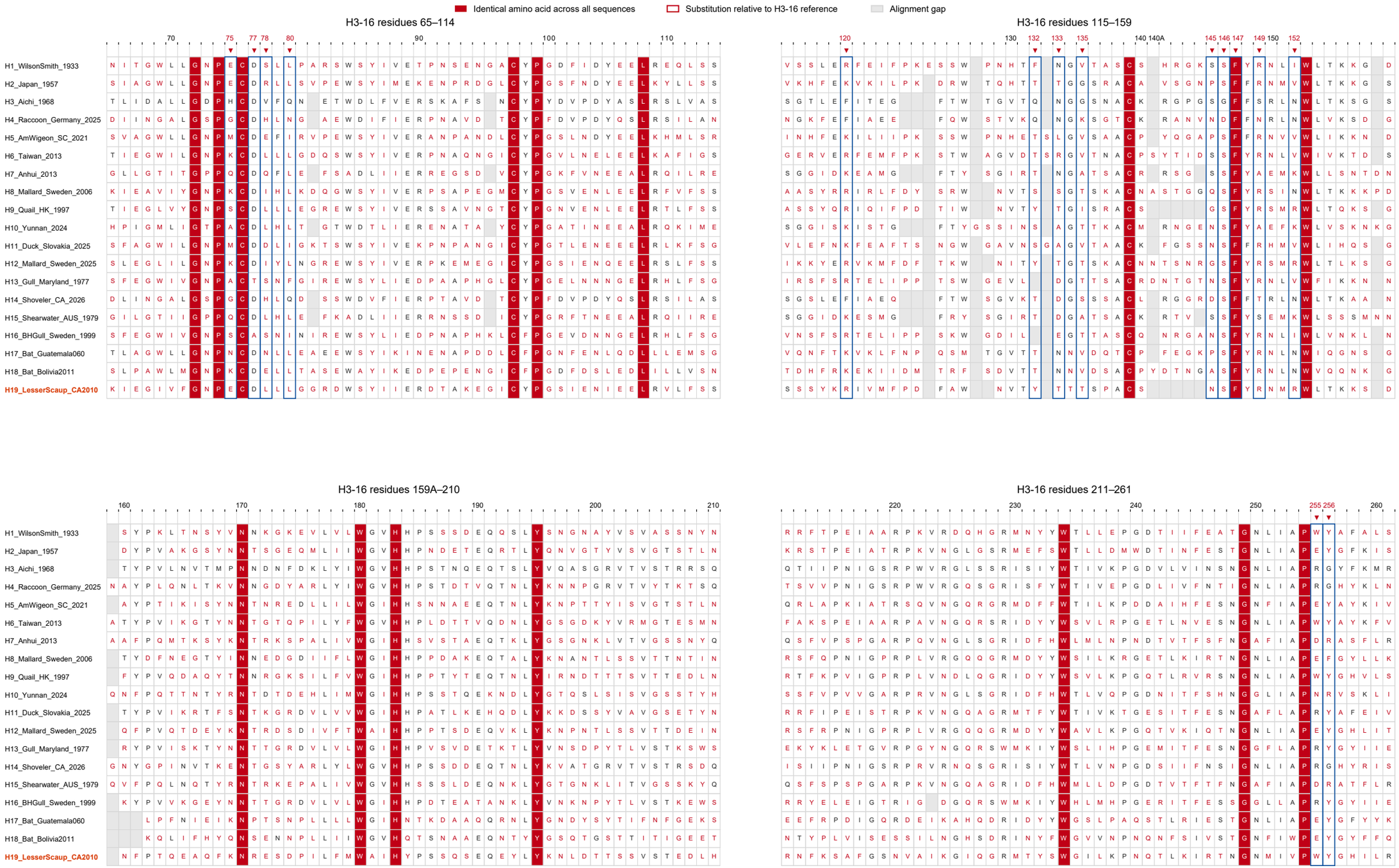


Figure S7

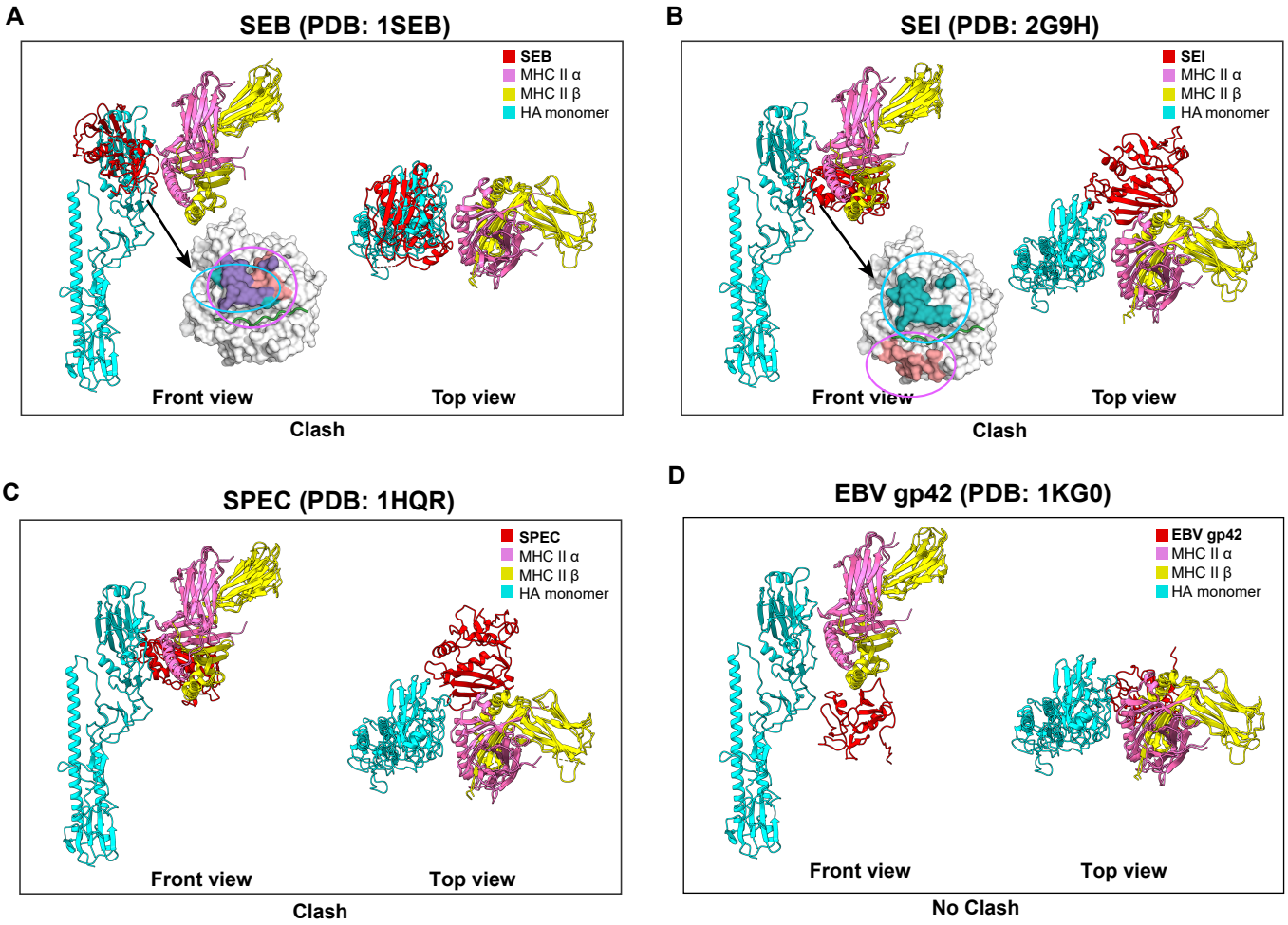

A
SEB (PDB: 1SEB)
SEB
MHC II α
MHC II β
HA monomer
Front view
Top view
Clash
B
SEI (PDB: 2G9H)
SEI
MHC II α
MHC II β
HA monomer
Front view
Top view
Clash
C
SPEC (PDB: 1HQR)
SPEC
MHC II α
MHC II β
HA monomer
Front view
Top view
Clash
D
EBV gp42 (PDB: 1KG0)
EBV gp42
MHC II α
MHC II β
HA monomer
Front view
Top view
No Clash

Table S1. Cryo-EM data processing and refinement statistics

Data Collection & Processing	H19/H2-E	Apo H19
Microscope	Titan Krios	Titan Krios
Camera	G4	G4
Magnification	×165,000	×165,000
Voltage (kV)	300	300
Total dose (e^{-}/Å^2)	50	50
Defocus range (μm)	-1.0 to -2.2	-1.0 to -2.2
Pixel size, Å per pixel	0.729	0.729
Symmetry imposed	C1	C3
Final particles images	1,054,740	146,408
Map resolution (Å, FSC=0.143)	2.65	2.67
Refinement		
Initial model used (PDB code)		
Non-hydrogen atoms	14,857	11748
Protein residues	1,822	1440
Validation		
Clash score	6.29	11.92
Poor rotamers (%)	2.97	0.00
R.m.s. deviations		
Bond lengths (Å)	0.002	0.007
Bond angles (°)	0.489	0.929
Ramachandran statistics (%)		
Most favored	96.29	94.40
Allowed	3.55	5.60
Outliers	0.17	0.00

Table S2. Intermolecular contacts between H19 HA and H2-E

H19	**H2-E**
E75	K18 (2)
D77	A61 (1), A64 (4), L60 (4)
L78	A64 (11), V65 (3)
L80	Q57 (3), L60 (3)
R120	Q57 (9, **1**)
Y132	E40 (7, **1**)
T133	K38 (13), E40 (6)
T135	E37 (3), K38 (1)
N145	E37 (5)
S146	I36 (1), E37 (13, **1**)
F147	E37 (1)
R149	I36 (6, **2**), E37 (2), K38 (1), S39 (3), Q57 (2), L60 (7)
R152	K38 (5, **1**), S39 (6, **1**)
W255	Q57 (4), S39 (6)
Y255a	E55 (3, **1**), Q57 (10)
Total	145, **8**

The first numbers indicate the number of vdw contacts between the pairs of residues. The underlined numbers indicate the number of potential H-bonds between the pairs of residues. The vdw contacts were analyzed at a cutoff of 4.5 Å. H-bonds were calculated using PDBePISA with a cutoff of 3.5 Å.